CONCENTRATION FLUCTUATIONS IN ADMS 3 ONWARDS, INCLUDING FLUCTUATIONS FROM ANISOTROPIC AND MULTIPLE SOURCES

The Met. Office (D J Thomson) and CERC

This document refers to ADMS versions 3, 4, 5 and 6.

Summary

This paper describes a revision of the scheme used to predict fluctuations from single point sources (P13/01, P13/02, P13/03 and P13/04) so as to address the problem of predicting fluctuations from anisotropic and multiple sources. Other changes between the ADMS 2 and ADMS 3 schemes are also summarised and some of the schemes are presented.

1. Introduction

This paper describes a revision of the scheme presented in P13/01, P13/02, P13/03 and P13/04 with the aim of predicting fluctuations for the wider range of source configurations which were introduced in ADMS 2, namely line, area, volume and multiple sources. Other changes between the ADMS 2 and ADMS 3 schemes are also summarised in this paper and some tests of the scheme are presented. The scheme in ADMS 6 is identical to that in ADMS 3, ADMS 4 and ADMS 5 except that it can now be used in conjunction with the buildings module.

There are two main scientific aspects to the revision. These concern the ability to calculate fluctuations for sources with different source length scales in the vertical and crosswind directions, and the ability to estimate the covariance of fluctuations from pairs of sources. Taken together these allow us in principle to estimate fluctuations for all desired source configurations. To treat an arbitrary source configuration, one can represent it as a collection of point, crosswind line and crosswind-vertical area sources. Once this is done, one has a collection of sources for which, with the ability to treat sources with different source length scales in the vertical and crosswind directions and to estimate the concentration covariance for pairs of sources, one can estimate the overall concentration variance (which is of course the sum of the variances from all the individual sources plus twice the sum of

the covariances from all the pairs of sources). One can then estimate the probability distribution of the concentration by assuming a 'clipped-normal' distribution as in ADMS 1 and 2 (see P13/01, §6).

As in P13/01 we consider three types of scenario corresponding to (i) continuous releases with the averaging time for concentration t_{av} specified by the user, (ii) time-integrated quantities from finite duration releases, and (iii) instantaneous quantities from finite duration releases. The fluctuations module in ADMS 3 onwards does not allow these types to be mixed in a single calculation. Also area, volume, line and multiple sources can be treated only for case (i). For cases (ii) and (iii) only point sources can be treated.

Note that the caveats in §1 and §2 of P13/01 regarding the degree of confidence that we have in the model apply here also and, again as mentioned in §1 of P13/01, the scheme is restricted to cases where there is an appreciable mean wind with $U \gg \sigma_u$.

The philosophical questions ('What do we mean by concentration?' and 'About what do the fluctuations fluctuate?' etc) discussed in §2 of P13/01 and in P13/03 will not be addressed here except to note that we follow the approach used in ADMS 2.

The calculation of long term climatological concentration statistics in a way which accounts for fluctuations is not addressed here but is covered in P07/05.

The structure of the rest of this paper is as follows. In §2 the notation and framework for analysis is presented. §3 describes a scheme to estimate the concentration variance for single sources and the concentration covariance for source pairs in idealised homogeneous stationary flows. §4 discusses how the ideas in §3 can be used to model the variance in more realistic atmospheric boundary layer flows. In §5 the interactions with other modules are described. As a result of the modifications to treat multiple and aniostropic sources and some other changes, the predictions with the new scheme are not always identical to those from the old scheme even in situations where the old scheme is applicable. These differences are summarised in §6. Some tests of the scheme (which, as noted above, is slightly different from the previous scheme, even for cases where the previous scheme was applicable) are presented in §7 and the tuning of the various tunable constants in the scheme is discussed. These tests of the new scheme include some test cases which were used in testing the previous scheme and which were reported in P13/02. Comparisons between the results presented here and those presented in P13/02 show reasonable agreement between the old and new schemes with only one case showing a significant difference (namely a somewhat different decay rate of concentration variance with averaging time – see figure 7 below and the equivalent figure in P13/02), but of course it must be remembered that the tests do not cover the entire range of possible scenarios. Finally the interface with the rest of ADMS is described in the appendix. This paper is not intended as a complete description of the fluctuations module and should be read in conjunction with the other ADMS papers on fluctuations (P13/01 and P13/03 in particular).

2. Notation and framework for analysis

Because of the relation between particle pairs and second moments of concentration, particle pairs will play a central role in our approach. We will use $\mathrm{X}_1(t)$ and $\mathrm{X}_2(t)$ to denote the trajectories of a pair of particles. It is sometimes convenient to express X_1 and X_2 in a manner related to the separation and centre of mass of the pair of particles. To this end we will write, following Durbin (1980), $\mathrm{X}_\Delta = (\mathrm{X}_1 - \mathrm{X}_2)/\sqrt{2}$ and $\mathrm{X}_\Sigma = (\mathrm{X}_1 + \mathrm{X}_2)/\sqrt{2}$. In the current context it might be more convenient to define X_Δ and X_Σ as the particle separation and centre of mass. However the additional factors of $\sqrt{2}$ are convenient in other contexts and we retain them for consistency with other work. In general when a given symbol appears with subscripts 1, 2, Δ and $\sum$, these quantities are to be interpreted as related by $(-)_\Delta = ((-)_1 - (-)_2)/\sqrt{2}$ and $(-)_\Sigma = ((-)_1 + (-)_2)/\sqrt{2}$.

We regard $\mathbf{X}_1(t)$ and $\mathbf{X}_2(t)$ as random variables in the usual way and, for any random vectors **A** and **B** derived from $\mathbf{X}_1(t)$ and $\mathbf{X}_2(t)$ we use $p_{\mathbf{A}|\mathbf{B}}(a|b)$ to indicate the probability density function of **A** conditional on $\mathbf{B} = b$. Ensemble averages will be denoted by angle brackets or sometimes, in the interests of compact notation, by overbars. $\mathbf{S}_{\mathbf{A}|\mathbf{B}=b}$ will denote the covariance matrix of the matrix of the random vector **A**, i.e. $\langle(\mathbf{A} - \langle\mathbf{A}\rangle)\rangle \otimes (\mathbf{A} - \langle\mathbf{A}\rangle)\rangle$ conditional on $\mathbf{B} = b$ Here $\otimes$ denotes a tensor product, so that, for example, $\mathbf{A} \otimes \mathbf{B}$ is the tensor **T** with components given by $T_{ij} = A_i B_j$. As an example, consider $\mathbf{S}_{\mathbf{X_1}(s)|\mathbf{X_1}(t)=\mathbf{x}}$. This is the covariance matrix of the distribution at time s of the particles which were at position **x** at time t. Similarly $\mathbf{S}_{\mathbf{AA'}|\mathbf{B}=b}$ denotes $\langle(\mathbf{A} - \langle\mathbf{A}\rangle)\otimes(\mathbf{A'} - \langle\mathbf{A'}\rangle)\rangle$, again conditional on $\mathbf{B} = b$. In general we will be interested in the concentration statistics at a particular place **x** and time t. In this case the conditioning $\mathbf{X}_1(t) = \mathbf{X}_2(t) = \mathbf{x}$ is implied if no conditioning is explicitly stated. We also use the shorter notations $\mathbf{S}_1$, $\mathbf{S}_\Delta$ and $\mathbf{S}_\Sigma$ for the covariance matrices of the displacement of a single particle, the change in the particle separation $(/\sqrt{2})$ and the change in the particle centre of mass $(\times\sqrt{2})$, i.e. $\mathbf{S}_1(s) = \mathbf{S}_{\mathbf{X}_1(s)}$, $\mathbf{S}_\Delta(s) = \mathbf{S}_{\mathbf{X}_\Delta(s)}$ and $\mathbf{S}_\Sigma(s) = \mathbf{S}_{\mathbf{X}_\Sigma(s)}$.

The various **S** matrices will usually be diagonal in our preferred frame of reference. In this case the various components will be denoted by σ^2 so that, for example, we have

$$\mathbf{S}_1 = \begin{pmatrix} \sigma_{1x}^2 & 0 & 0 \\ 0 & \sigma_{1y}^2 & 0 \\ 0 & 0 & \sigma_{1_z}^2 \end{pmatrix}$$

and

$$\mathbf{S}_\Delta = \begin{pmatrix} \sigma_{\Delta x}^2 & 0 & 0 \\ 0 & \sigma_{\Delta y}^2 & 0 \\ 0 & 0 & \sigma_{\Delta_z}^2 \end{pmatrix}$$

All sources will be assumed to have a Gaussian shape. This assumption is of course unlikely to be accurate in practice, but an attempt at a more precise description seems unwarranted in view of the uncertainties associated with source effects. It would be possible, in principle, to represent a source distribution more accurately by representing it as a combination of several smaller (Gaussian) sources. It might even be possible to do the integrals in §3 below for a wider variety of shapes, but we will not explore this here.

We will use $G_\lambda(\mathbf{x}, \mathbf{S})$ to denote a λ-dimensional Gaussian distribution with covariance matrix **S.** We note that the deductions in §3 below require a number of integrals of Gaussian distributions. In general these are most easily carried out, not analytically from first principles, but by using general properties of Gaussian distributions such as the convolution property

$$\int G_\lambda(\mathbf{x}-\mathbf{y}, \mathbf{S}) G_\lambda(\mathbf{y}-\mathbf{z}, \mathbf{S}') d\mathbf{y} = G_\lambda(\mathbf{x}-\mathbf{z}, \mathbf{S}+\mathbf{S}')\big)$$

which reflects the fact that the sum of two independent Gaussian random variables is Gaussian with mean and variance given by the sum of the means and variables of the two random variables.

3. Second moments of concentration in homogeneous stationary turbulence

We start by considering the idealised case of instantaneous sources in stationary homogeneous turbulence with no mean velocity. The idea behind considering this case is that, as often done in such situations, the dispersion as a function of time in this flow can be regarded, via a Taylor-type transformation, as approximating the dispersion as a function of downwind distance divided by wind speed in a flow with an appreciable mean wind. As an example the dispersion in time from a line source can be regarded as an approximation to the dispersion with downwind distance from a point source in a mean wind (the wind direction and the line source in the two flows being in the same direction). See Townsend (1954) for a discussion of the similar situation involving instantaneous area and continuous cross-wind line sources.

Because we consider only instantaneous sources, the results are, when translated to situations with an appreciable mean wind, directly applicable only to sources with no along wind extent. The approach can however be extended to treat sources with an along wind extent either by ignoring the along wind extent, or by splitting the source into subsources as described in §1 and §4.

For a single source, the second moments of the concentration field $\mathrm{c}(\mathbf{x}, t)$ for a source released at time s are given by

$$\overline{c(\mathbf{x},t)c(\mathbf{x},t)} = \int \boldsymbol{p}_{\mathbf{x}_1(s),\mathbf{x}_2(s)}(\mathbf{y}_1,\mathbf{y}_2) q(\mathbf{y}_1) q(\boldsymbol{y}_2) d\boldsymbol{y}_1 d\boldsymbol{y}_2 \qquad (1)$$

where $q(\mathbf{x})$ is the source distribution as a function of position. In applying this result we adopt an approximation introduced by Sawford (1983). Sawford argued that, if we follow the particles backwards in time from time t to time s, the displacement of the centre of mass of particle pairs is close to Gaussian and independent of the particle separation. For a Gaussian source centred on $\mathbf{y}$ with integrated source strength (total mass released) Q and with source distribution covariance matrix $\mathbf{S}_0$ $\left(\text{so that } q(\mathbf{x}) = QG_3(\mathbf{x}\text{-}\mathbf{y}, \mathbf{S}_0)\right)$ this leads to the result

$$\overline{c^2}(\mathbf{x}) = Q^2 G_3\left((\mathbf{x}-\mathbf{y})\sqrt{2}, \mathbf{S}_\Sigma + \mathbf{S}_0\right) \int p_{\mathbf{X}_\Delta(s)}(\mathbf{y}_\Delta)\, G_3(\mathbf{y}_\Delta, \mathbf{S}_0) d\mathbf{y}_\Delta. \qquad (2)$$

Note that when $p_{\mathbf{X}_\Delta(s)}$ is Gaussian, the integral in (2) is equal to $G_3(0, \mathbf{S}_\Delta + \mathbf{S}_0)$. Theory and random walk simulations show that $p_{\mathbf{X}_\Delta(s)}$ is actually more peaked than Gaussian, resulting in an additional contribution to $\overline{c^2}$. We will write the integral in (2) as $\mu G_3(0, \mathbf{S}_\Delta + \mathbf{S}_0)$, where μ is a factor related to the non-Gaussianity of $p_{\mathbf{X}_\Delta(s)}$. This leads to

$$\overline{c^2}(\mathbf{x}) = Q^2 \mu G_3\left((\mathbf{x}-\mathbf{y})\sqrt{2}, \mathbf{S}_\Sigma + \mathbf{S}_0\right) G_3(0, \mathbf{S}_\Delta + \mathbf{S}_0). \qquad (3)$$

In conjunction with the Sawford approximation, it is natural, in homogeneous turbulence, to make a Gaussian assumption for the mean concentration:

$$\bar{c}(\mathbf{x}) = QG_3(\mathbf{x}-\mathbf{y}, \mathbf{S}_1 + \mathbf{S}_0). \qquad (4)$$

Let us now consider two instantaneous sources at times s_1 and s_2. We consider two distinct times s_1 and s_2 here since once we transform from time to downwind distance divided by wind speed as discussed above, this will enable us to treat sources which are separated in the along wind as well as in the crosswind or vertical directions. Suffixes 1 and 2 will be used to denote properties associated with each of the two sources. For example, as well as s_1 being the release time for source 1, we will use c_1 to indicate the concentration resulting from source 1 and q_1 to denote the source distribution 1. The equivalent result to (1) is

$$\overline{c(\mathbf{x},t)c(\mathbf{x},t)} = \int p_{\mathbf{X}_1(s_1),\mathbf{X}_2(s_2)}(\mathbf{y}_1,\mathbf{y}_2)q_1(\mathbf{y}_1)q_2(\mathbf{y}_2)d\mathbf{y}_1 d\mathbf{y}_2.$$

In applying this result we extend Sawford's approximation by making the assumption that, if we follow the particles backwards in time from time t, the displacements of the centres of mass of particles pairs at time s_1 and s_2 are jointly Gaussian and independent of the particle separations at times s_1 and s_2. As with Sawford's original approximation, the joint Gaussianity of the centres of mass is likely to be reasonably accurate because the centre of mass motions are dominated by the energy-containing eddies, while the independence assumption is supported by the fact the variables concerned are uncorrelated. (We note that an alternative extension of Sawford's approximation based on assuming the independence of $\mathbf{X}_1(s_1) - \mathbf{X}_2(s_2)$ and $\mathbf{X}_1(s_1) + \mathbf{X}_2(s_2)$ is not appropriate because $\mathbf{X}_1(s_1) - \mathbf{X}_2(s_2)$ and $\mathbf{X}_1(s_1) + \mathbf{X}_2(s_2)$ are in general correlated. For the case $s_1 = s_2$ no extension of Sawford's approximation is needed and our extension reduces to Sawford's original approximation.) For Gaussian sources this leads to an expression analogous to (2) although considerably more complex. For our purposes it is simplest to pass directly to the expression analogous to (3) which results when we (i) assume the particle separations at times s_1 and s_2 are jointly Gaussian and (ii) introduce a factor μ_{12} to represent the non-Gaussianity of $p_{\mathbf{X}_\Delta(s_1),\mathbf{X}_\Delta(s_2)}$. For Gaussian sources centred on $\mathbf{y}_1$ and $\mathbf{y}_2$ with integrated source strengths Q_1 and Q_2 and with source distribution covariance matrices $\mathbf{S}_{01}$ and $\mathbf{S}_{02}$, this leads to the result

$$\overline{c_1 c_2}(\mathbf{x}) = Q_1 Q_2 \mu_{12} G_6\left((\mathbf{y}_1 - \mathbf{x}, \mathbf{y}_2 - \mathbf{x}), \begin{pmatrix} \mathbf{S}_{\mathbf{X}_1(s_1)} + \mathbf{S}_{01} & \mathbf{S}_{\mathbf{X}_1(s_1)\mathbf{X}_2(s_2)} \\ \mathbf{S}_{\mathbf{X}_1(s_1)\mathbf{X}_2(s_2)} & \mathbf{S}_{\mathbf{X}_2(s_2)} + \mathbf{S}_{02} \end{pmatrix}\right) \quad (5)$$

Note that the result for a single source can be expressed in the analogous form

$$\overline{c^2}(\mathbf{x}) = Q^2 \mu G_6\left((\mathbf{y} - \mathbf{x}, \mathbf{y} - \mathbf{x}), \begin{pmatrix} \mathbf{S}_1(s) + \mathbf{S}_0 & \mathbf{S}_{\mathbf{X}_1(s)\mathbf{X}_2(s)} \\ \mathbf{S}_{\mathbf{X}_1(s)\mathbf{X}_2(s)} & \mathbf{S}_1(s) + \mathbf{S}_0 \end{pmatrix}\right) \quad (6)$$

showing, as expected, that the single source result is a special case of the two source result obtained by putting $c_1 = c_2 = c,\ Q_1 = Q_2 = Q, \mu_{12} = \mu,\ \mathbf{y_1} = \mathbf{y_2} = \mathbf{y},\ s_1 = s_2 = s,\ \ \mathbf{S}_{01} = \mathbf{S}_{02} = \mathbf{S}_0$ and $\mathbf{S}_{\mathbf{x}_1(s_1)} = \mathbf{S}_{\mathbf{x}_2(s_2)} = \mathbf{S}_1(s)$. The expression (6) is equivalent to (3) but can be derived more simply by making the joint Gaussian assumption at the outset as we did in deriving (5). The expression (3) in terms of separation and centre of mass coordinates is more convenient however because of the fact that, in these coordinates, the Gaussian factorises into two Gaussians. It is a general property of much of the following analysis that the one-source results are a

special case of the two-source results but, because of the aim of expressing the one-source results as simply as possible, this is not always immediately apparent from the form of the equations.

Some light can be shed on the above equations and, in particular, on the quantities μ and μ_{12} by comparing the equations with the results obtained from Gifford's (1959) fluctuating (meandering might be a better word – there are no in-plume fluctuations) plume model (see also Sykes (1984)). Gifford assumed a Gaussian instantaneous plume with no internal fluctuations which meanders with the plume centroid position varying randomly according to a Gaussian distribution (see figure 1 (a)). In the current instantaneous-source context we consider Gaussian puffs (one or two according to whether we are considering one or two sources) without internal fluctuations and with centroid positions varying between realisations according to a Gaussian distribution (or, for two sources, a joint Gaussian distribution). $\mathbf{S}_i$ will denote the covariance matrix of the concentration distribution within such a puff and $\mathbf{M}$ will denote the position of the puff centroid. This leads to

$$\overline{c^2}(\mathbf{x}) = Q^2 G_3\left((\mathbf{x}-\mathbf{y})\sqrt{2}, \mathbf{S}_i + 2\mathbf{S}_{\mathbf{M}}\right) G_3(0, \mathbf{S}_i) \tag{7}$$

for one source and

$$\overline{c_1 c_2}(\mathbf{x}) = Q_1 Q_2 G_6\left((\mathbf{y}_1 - \mathbf{x}, \mathbf{y}_2 - \mathbf{x}), \begin{pmatrix} \mathbf{S}_{i1} + \mathbf{S}_{\mathbf{M}_1} & \mathbf{S}_{\mathbf{M}_1\mathbf{M}_2} \\ \mathbf{S}_{\mathbf{M}_1\mathbf{M}_2} & \mathbf{S}_{i2} + \mathbf{S}_{\mathbf{M}_2} \end{pmatrix}\right) \tag{8}$$

for two sources. These equations have the same form as the results obtained using the Sawford approximation (equations (3), (5) and (6)) if we take μ and μ_{12} to be unity in the Sawford approximation. (Note we have chosen to express the one-source result in a form analogous to (3) rather than (6) but it can be re-expressed in a form similar to (6).) We would like to conclude that the departure of μ and μ_{12} from unity reflects in-puff fluctuations (or in-plume fluctuations if we consider a line source and interpret it as a continuously emitting point source via the Taylor-type transformation discussed above). However this is not quite true. Firstly $\mathbf{S}_{\mathbf{X}_1(s_1)\mathbf{X}_2(s_2)}$ in (5) is not in general equal to $\mathbf{S}_{\mathbf{M}_1\mathbf{M}_2}$ in (8). This is easy to see because $\mathbf{S}_{\mathbf{M}_1\mathbf{M}_2}$varies with $\mathbf{y}_1 - \mathbf{y}_2$ while $\mathbf{S}_{\mathbf{X}_1(s_1)\mathbf{X}_2(s_2)}$ doesn't. Secondly, even for a single source we have $\mathbf{S}_i \neq \mathbf{S}_0 + \mathbf{S}_\Delta$. This is because, near the source where size is important, we expect $\mathbf{S}_i$ to grow from $\mathbf{S}_0$ faster than $\mathbf{S}_\Delta$ grows from zero – particles on opposite sides of the source (which contribute to $\mathbf{S}_i$) can separate as a result of velocity differences across the source while initially close particles (which contribute to $\mathbf{S}_\Delta$) can only separate due to the smallest eddies. Even at larger times when source size is forgotten, we expect $\mathbf{S}_i$ to equal the forward separation covariance matrix $\mathbf{S}_{\mathbf{X}_\Delta(t)|\mathbf{X}_\Delta(s)=0}$ not the backward one $\mathbf{S}_{\mathbf{X}_\Delta(s)|\mathbf{X}_\Delta(t)=0}$ (that it does equal the forward one is a classical result, Batchelor (1952)). It is possible however to formulate the fluctuating puff model in the backwards direction (see figure 1(b)) and it is true to say that the Sawford approximation to backwards dispersion with $p_{\mathbf{X}_\Delta(s)}$ or $p_{\mathbf{X}_\Delta(s_1),\mathbf{X}_\Delta(s_2)}$ assumed Gaussian (or equivalently simply approximating $p_{\mathbf{X}_1(s),\mathbf{X}_2(s)}$ or $p_{\mathbf{X}_1(s_1),\mathbf{X}_2(s_2)}$ directly by a Gaussian) is exactly equivalent to making a Gifford-type fluctuating puff assumption for the backwards dispersion (i.e. to assuming backwards travelling Gaussian puffs originating from a point source at $\mathbf{x}$ at time t and varying between realisations only

through Gaussian displacements of their centroids). If we accept that the errors in the Sawford approximation and in assuming Gaussian centroid displacements and a Gaussian shape for the mean instantaneous puff (i.e. for the mean of the centroid-aligned puffs) are small, then we can say that the departure of μ and μ_{12} from unity reflects in-puff fluctuations in the *backwards* puff.

For completeness we note that the above extends easily to two-point moments $\overline{c(\mathbf{x_1})c(\mathbf{x_2})}$ The backwards fluctuating puff model then of course involves two puffs starting at $\mathbf{x}_1$ and $\mathbf{x}_2$. The fact that the Sawford approximation has a clearer relation to the backwards fluctuating puff model than to the forwards model is perhaps not surprising because the Sawford approximation is formulated in terms of backwards dispersion. There is of course (by symmetry) a similar relation between the forward Sawford approximation and the forward fluctuating puff model if we restrict ourselves to point sources with $s_1 = s_2$ (but allow the possibility of volume average concentrations, possibly at two times). It seems unlikely however that any such clear relationship is possible for the forwards Sawford approximation from extended sources or for the backwards Sawford approximation with volume average concentrations – both cases involve integrations over values of the 'initial' (i.e. the conditioning) particle separation and so are analytically rather intractable. In addition it is unclear how a Sawford-type approximation might be formulated with two conditioning times. These problems are the reason we use the backwards Sawford approximation here – we wish to be able to treat extended sources with $s_1 \neq s_2$ easily and are not so concerned about volume averaging effects or two time (or indeed two-point) moments. (We do however have *some* interest in time averaged fluctuations. Because of the above the treatment of these is rather messy – see below.)

As well as providing some insight into the significance of μ and μ_{12} the fluctuating plume approach is useful for showing that our approach will predict positive variance and correlations lying between ± 1.

By using some simple assumptions, $\overline{c^2}$ and, for two sources, $\overline{c_1 c_2}$ can be expressed more simply. Our aim here is to express $\overline{c^2}$ and $\overline{c_1 c_2}$ in terms of the $\overline{c}$ -field (or $\overline{c_1}$ and $\overline{c_2}$ fields) and as few extra quantities as possible. The reason for this is to provide a basis for modelling concentration variance in more complex flows, in particular in flows where the mean concentration distribution is non-Gaussian. We assume the various **S** matrices are diagonal in a frame with coordinates x, y, z. This leads to

$$\overline{c^2} = \mu \bar{c}_m^2 g_x g_y g_z f_x f_y f_z \tag{9}$$

for one source and

$$\overline{c_1 c_2} = \mu_{12} \overline{c}_{1m} \overline{c}_{2m} g_x g_y g_z f_x f_y f_z \tag{10}$$

for two sources. Here $\bar{c}_m$ is the spatial peak concentration, the g factors relate the overall level of the second order moments to the first order moments, and the f factors describe the spatial variation of the second order moments. For the one source case

$$g_x^2 = \frac{(\sigma_{1x}^2 + \sigma_{0x}^2)^2}{(\sigma_{\Delta x}^2 + \sigma_{0x}^2)(\sigma_{\Sigma x}^2 + \sigma_{0x}^2)} \tag{11}$$

and

$$f_x = h_x^{\chi_x} \tag{12}$$

where

$$\chi_s = 2\,\frac{\sigma_{1x}^2 + \sigma_{0x}^2}{\sigma_{\Sigma x}^2 + \sigma_{0x}^2}. \tag{13}$$

g_y, g_z, f_y and f_z are defined similarly. h_x, h_y and h_z are the 'shape factors' corresponding to the way the concentration falls off in the x, y and z directions, and are defined so that $\overline{c} = \overline{c}_m h_x h_y h_z$. These equations correspond to equations (5) to (10) in P13/01, although they are expressed a little differently. We note that the components of σ_Σ can be expressed as

$$\sigma_\Sigma^2 = 2\sigma_1^2 - \sigma_\Delta^2 \tag{14}$$

For the two source case we have

$$g_x^2 = \frac{ac}{ac - b^2} \tag{15}$$

and

$$f_x = (h_{1x}h_{2x})^{\chi_x} \exp\left(-\beta_x \sqrt{\log h_{1x} \log h_{2x}}\right) \tag{16}$$

where

$$\chi_x = \frac{ac}{ac - b^2} (= g_x^2) \tag{17}$$

and

$$\beta_x = -\frac{2b\sqrt{ac}}{ac - b^2}\,\text{sign}_x \tag{18}$$

with

$$a = \sigma_1^2(s_1) + \sigma_{01}^2 \tag{19}$$

$$b = \sigma^2_{\mathbf{X}_{1(s_1)}\mathbf{X}_{2(s_2)}} \tag{20}$$

and

$$c = \sigma_1^2(s_2) + \sigma_{02}^2 \tag{21}$$

where we have suppressed the suffix x in these last equations for clarity. sign_x equals 1 if the output point lies outside the sources in the x-direction and -1 if the output point lies between the sources.

For the one source case (equation (9) and equations (11) to (14)), $\overline{c^2}$ is determined by the $\overline{c}$ -field, by the x, y and z components of $\sigma_1(s)$, $\sigma_\Delta(s)$ and σ_0, and by μ. For the two source case (equation (10) and equations (15) to (21)), $\overline{c_1 c_2}$ is determined by the $\overline{c_1}$ and $\overline{c_2}$ fields, by the x, y and z components of $\sigma_1(s_1)$, $\sigma_1(s_2)$, $\sigma^2_{\mathbf{X}_1(s_1)\mathbf{X}_2(s_2)}$, σ_{01} and σ_{02}, and by μ_{12}.

We will now consider the problem of determining σ_Δ. Consider first short travel times, where the separation of particles pairs is dominated by inertial subrange eddies. This range of travel times can be characterised by $\sigma_\Delta \ll \sigma_1$ or, equivalently, $t\text{-}s \ll T_L$ (where T_L is the Lagrangian time scale). In this region inertial subrange theory predicts that $p_{\mathbf{X}_\Delta}$ grows self-similarly and isotropically, with σ_Δ^2 growing in proportion to $\varepsilon(t-s)^3$. The random walk simulations of Thompson (1990), which show reasonable agreement with measurements of concentration fluctuations, indicate that

$$\sigma_\Delta^2 \simeq \varepsilon(t-s)^3/3.$$

At large times $\mathbf{S}_1 \simeq \mathbf{S}_\Delta$ with both growing linearly with t. In ADMS 1 and 2 we interpolated between these limiting cases by using

$$\frac{1}{\sigma_\Delta} = \frac{1}{\sigma_1} + \frac{1}{(\varepsilon(t-s)^3/3)^{1/2}}$$

This formula performed quite well, although it resulted in σ_c values which were perhaps a little on the high side (see P13/02). In fact there is little theoretical reason to prefer one interpolation over another and retaining the same formula is not likely to preserve the previous (fortuitously) good performance because of other changes to the fluctuations scheme. Hence we adopt an interpolation formula which gives some scope for tuning, namely

$$\sigma_\Delta^2 = \frac{\sigma_1^2 R^2}{\sigma_1^2 + A_0\sigma_1 R + R^2} \tag{22}$$

where $R^2 = \varepsilon(t-s)^3/3$ and A_0 is a tunable constant lying in the range (0,2). $A_0 = 2$ corresponds to the previous approach while $A_0 = 0$ corresponds to a similar interpolation using squared quantities, i.e.

$$\frac{1}{\sigma_\Delta^2} = \frac{1}{\sigma_1^2} + \frac{1}{\varepsilon(t-s)^3/3}$$

(22) is applied separately to the x, y and z components.

The selection of a model for μ is more complicated. In P13/01 we presented a model suitable for point and line sources and we extend this to area sources using the same methodology. For infinite area sources we take μ to equal μ_A defined as the minimum of

$$\begin{cases} 1 & \sigma_\Delta/\sigma_0 \le 0.7 \\ 1 + 0.4\log((\sigma_\Delta/\sigma_0)/0.7)/\log(9/0.7) & 0.7 \le \sigma_\Delta/\sigma_0 \le 9 \\ 1.4 & 9 \le \sigma_\Delta/\sigma_0 \end{cases} \quad (23)$$

and

$$\max(1, 1.4 - (0.4/3)t\varepsilon/\sigma_{vel}^2) \quad (24)$$

Here σ_{vel}^2 is the average of the variances of the three components of velocity. For infinite line sources we take μ to equal μ_L defined as the minimum of

$$\begin{cases} 1 & \sigma_\Delta/\sigma_0 \le 0.9 \\ 1 + 1.8\log((\sigma_\Delta/\sigma_0)/0.9)/\log(17/0.9) & 0.7 \le \sigma_\Delta/\sigma_0 \le 17 \\ 2.8 & 17 \le \sigma_\Delta/\sigma_0 \end{cases} \quad (25)$$

and

$$\max(1, 2.8 - 0.6\, t\varepsilon/\sigma_{vel}^2) \quad (26)$$

For isotropic point sources we take μ to equal μ_p defined as the minimum of

$$\begin{cases} 1 & \sigma_\Delta/\sigma_0 \le 1 \\ 1 + 11\log((\sigma_\Delta/\sigma_0)/1)/\log(100/1) & 1 \le \sigma_\Delta/\sigma_0 \le 100 \\ 12 & 100 \le \sigma_\Delta/\sigma_0 \end{cases} \quad (27)$$

and

$$\max(1, 12 - (11/3)t\varepsilon/\sigma_{vel}^2) \quad (28)$$

We now need to consider more general sources. An appropriate expression for μ with the right qualitative properties can be obtained as follows. Consider the three components of σ_Δ/σ_0, namely $\sigma_{\Delta x}/\sigma_{0x}$, $\sigma_{\Delta y}/\sigma_{0y}$ and $\sigma_{\Delta z}/\sigma_{0z}$ Set $(\sigma_\Delta/\sigma_0)_A$ equal to the largest component (i.e. the value most appropriate if the source is considered as an area source), $(\sigma_\Delta/\sigma_0)_L$ equal to the middle component and $(\sigma_\Delta/\sigma_0)_P$ equal to the smallest. Then evaluate μ_A using $(\sigma_\Delta/\sigma_0)_A$, μ_L using $(\sigma_\Delta/\sigma_0)_L$ and μ_P using $(\sigma_\Delta/\sigma_0)_P$ and take the largest of the three resultant μ values. It is easily checked that the value of μ obtained behaves appropriately. Consider, for example, an area source of finite area. At close range (where the source can be approximated by an infinite area source) μ will be given by μ_A, whereas at large distances (where the source can be approximated by a point source) μ will be given by μ_p.

We now need to consider the two source quantities $\sigma^2{}_{\mathbf{X}_1(s_1)\mathbf{X}_2(s_2)}$ and μ_{12}. If $s_1 = s_2 = s$ then $\sigma^2{}_{\mathbf{X}_1(s_1)\mathbf{X}_2(s_2)} = \sigma_1^2(s) - \sigma_\Delta^2(s)$. In general we take

$$\sigma^2{}_{\mathbf{X}_1(s_1)\mathbf{X}_2(s_2)} = \left(\left(\sigma_1^2(s_1) - \sigma_\Delta^2(s_1)\right)\left(\sigma_1^2(s_2) - \sigma_\Delta^2(s_2)\right)\right)^{1/2}$$

(evaluated separately for x, y and z components). This is consistent with straight line motion at small travel times and tends to zero at large travel times. μ_{12} is a little more complex. Inspired by the exact form for μ_{12} (analogous to the equation

$$\int p_{\mathbf{X}_\Delta(s)}(\mathbf{y}_\Delta) G_3(\mathbf{y}_\Delta, \mathbf{S}_0) d\mathbf{y}_\Delta = \mu G_3(0, \mathbf{S}_\Delta + \mathbf{S}_0)$$

for the one source μ) we re-evaluate the one source μ's for each source with σ_0^2 replaced (component-wise) by

$$\tfrac{1}{2}(\sigma_1(s_1) - \sigma_1(s_2))^2 + \tfrac{1}{2}(\sigma_{01}^2 + \sigma_{02}^2) + A_1 y_\Delta^2 \qquad (29)$$

and take μ_{12} equal to unity plus the geometric means of the two μ -1's. Note y_Δ here is the appropriate component of $\mathbf{y}_\Delta$, the source separation vector $\left(/\sqrt{2}\right)$. A_1 is a tunable constant.

The above gives us a model which expresses the (one-point) second moments of the concentration in terms of the turbulence statistics (σ_{vel}^2 and ε), travel time $t - s$ for each source, source properties (σ_0 components for each source and, for the multiple source case, y_Δ components for each pair of sources), and the mean concentration field ($\overline{c_m}$, shape factors h, and σ_1 components).

We now consider the problem of the effect of time averaging on the second moments of concentration (in the presence of a significant mean velocity). We adopt a somewhat different approach to that in ADMS 1 and 2 in order to provide for inertial-meander subrange behaviour (Thompson 1997) and in order to allow the possibility of negative correlations between concentrations from different sources becoming more negative as averaging time increases (this can occur if the instantaneous plumes are very intermittent and is hard to treat within the context of the simple damping used in ADMS 1 and 2). As in ADMS 1 and 2 we treat time averaging over a finite interval t_{av} only for type (i) scenarios – i.e. continuous releases or, in the Taylor transformed frame, instantaneous sources with infinite extent in the direction, x say, corresponding to the mean flow. In keeping with the view throughout most of this section, we work in the Taylor-transformed frame and so deal with averages over a distance $x_{av} = Ut_{av}$ in the x direction. Our approach is to allow for averaging time (i) by increasing the σ_Δ's to account for the widening of the time-averaged plume (or puff) and (ii) by damping the $\mu - 1$'s to account for the damping of 'in-plume' (or in-puff') fluctuations. Note we damp $\mu - 1$ rather than μ because it is the departure of μ from unity which represents the in-plume fluctuations. In detail we calculate a damping factor d_μ for μ-1 from

$$d_\mu = \frac{1}{1 + x_{av}/L_c} \qquad (30)$$

with L_c given by

$$\frac{1}{L_c} = \frac{1}{A_2(\varepsilon(t-s)^3)^{1/2}} + \frac{1}{A_3(\sigma_{vel}^3/\epsilon)} \tag{31}$$

L_c is the spatial scale of the 'in-plume' (or 'in-puff') fluctuations. We could probably do better here, e.g. by taking account of the inertial-convective subrange scaling of the in-plume fluctuations, but we wish to keep the model reasonably simple. We then calculate the effective σ_Δ for the averaged plume, $\hat{\sigma}_\Delta$, by modifying the equation (22) for σ_Δ to

$$\hat{\sigma}_\Delta^2 = \frac{\sigma_1^2 \hat{R}^2}{\sigma_1^2 + A_0\sigma_1\hat{R} + \hat{R}^2} \tag{32}$$

(applied component-wise) where

$$\hat{R}^2 = \varepsilon(t-s)^3/3 + (4C/27)\varepsilon^{2/3}x_{av}^{2/3}(t-s)^2 + (A_4\sigma_{vel}^2(t-s)^2 + A_5\varepsilon(t-s)^3)x_{av}^2\varepsilon^2/\sigma_{vel}^6 \tag{33}$$

C is the Kolmogorov constant in the longitudinal velocity structure function and is taken here to be 2. A_2, A_3, A_4 and A_5 are tunable constants. For $t \ll T_L$ and x_{av} much smaller than the integral scale of the turbulence, the second term in (33) dominates the difference between $\hat{\sigma}_\Delta$ and σ_Δ and is designed to give the correct inertial-meander subrange behaviour (Thompson 1997). For larger t or larger x_{av} the third term in (33) ensures that $\hat{\sigma}_\Delta$ approaches σ_1 as x_{av} increases beyond the integral scale of the turbulence. d_μ and $\hat{\sigma}_\Delta$ are calculated separately for each source. For each source we then calculate $\overline{c^2}$ using the $\hat{\sigma}_\Delta$ and a modified μ calculated as

$$\hat{\mu} = 1 + (\mu - 1)d_\mu. \tag{34}$$

For a pair of sources we calculate $\overline{c_1 c_2}$ using the $\hat{\sigma}_\Delta$'s for each source and a modified μ_{12} calculated as

$$\hat{\mu}_{12} = 1 + (\mu_{12} - 1)(d_{\mu 1}d_{\mu 2})^{1/2} \tag{35}$$

Finally we consider the problem of the statistics of time-integrated concentrations from a finite duration release (in the presence of a significant mean velocity). We treat this case for single sources only. In the Taylor-transformed frame this amounts to considering x-integrated concentrations for instantaneous sources with finite σ_{0x}. As in ADMS 1 and 2 we treat this by assuming a reciprocity relation – namely we assume that the statistics of the time-integrated concentration for a release of duration t_R are the same as those for the concentration integrated over t_{av} (i.e. t_{av} times the time-averaged concentration) from a continuous release with the same release rate for t_{av} equal to t_R. This reciprocity relation is not exact because turbulence is not

(statistically) invariant under time reversal. However any lack of symmetry here could only be accounted for in a much more sophisticated approach. Also it is not exact when source size is important – this is because we are swapping the t-extent of the source and receptor but not the spatial extent (or the x but not the y and z extents in the Taylor transformed frame). We treat only single sources for this case because, for multiple sources with different locations and release periods, applying the same idea would require us to estimate two-point (in space and time) concentration correlations.

Once the concentration variance has been estimated, the probability distribution of the concentration can be estimated by assuming a clipped normal distribution as in ADMS 1 and 2 (see P13/01). We truncate this at the 99.999th percentile to avoid very large concentrations.

4. Second moments of concentration in the atmospheric boundary layer

As discussed above, the dispersion in time from an instantaneous line source aligned with the x-direction in homogenous turbulence with no mean flow (i.e. the situation considered in §3 with $\sigma_{0x} = \infty$) can be regarded as an approximation to the downwind dispersion from a continuous point source in a homogeneous turbulent flow with mean velocity $U(\gg \sigma_u)$. If the line source is finite in length (due to σ_{0x} being finite) then it can be regarded as an approximation to a finite duration release. Hence, for continuous or finite duration releases in a homogeneous turbulent flow with a mean velocity, we can use results in §3.

In more realistic inhomogeneous atmospheric flows we follow the general philosophy of ADMS in using the results for idealised homogeneous flows, but with turbulence quantities evaluated at an appropriate location. At small travel times, when σ_Δ is dominated by inertial subrange eddies, this approach has strong theoretical justification. At very large travel times, much larger than the time-scales of the turbulent eddies controlling the plume spread, we expect fluctuations in reality to be dominated by changes in the 'mean wind direction'. We treat this by using a different value of σ_{1y} in estimating $\sigma_{\Delta y}$ than is used elsewhere. (More specifically, for zero averaging time, we use a value which reflects spread due to turbulence but excludes spread due to mean wind direction changes. This prevents $\sigma_{\Delta y}$ approaching the mean plume width and so retains fluctuations due to meandering caused by changes in the mean wind direction. As averaging time increases, the value of σ_{1y} used to estimate $\sigma_{\Delta y}$ increases towards the value used elsewhere to reflect the fact that the fluctuations due to changes in mean wind direction, like those due to turbulence, are smoothed out by time averaging.) For intermediate times our approach provides a plausible interpolation between these two limits for which, however, the ultimate justification is comparison with data.

In treating area, volume and line sources we split these into sub-sources consisting of crosswind line and crosswind-vertical area sources as described in P25/01, thus treating them as multiple sources. We follow the same splitting algorithm used for estimating the mean concentration.

In the following we describe in more detail the values adopted for the various inputs to the scheme described in §3. As discussed in the introduction, multiple sources and area, volume and line sources are treated for continuous releases only, and, for finite duration releases, we treat only point sources with zero or infinite averaging (or integrating) times.

4.1 Unaveraged concentrations for continuous and finite duration releases

Travel time $t\text{-}s$ is calculated as downwind distance/U (an approximation to the travel time).

U, ε and σ_{vel}^2 are evaluated at the mean plume height $\overline{z}$ at the point of interest (and not the height at which σ_c is required) with σ_{vel}^2 taken to be $(\sigma_u^2 + \sigma_v^2 + \sigma_w^2)/3$. They are evaluated for each plume separately – in particular different U, ε and σ_{vel}^2 are used at various places in multiple source calculations. It's mostly obvious which should be used – e.g. although the two source μ involves data from both plumes, $(t\text{-}s_1)\varepsilon/\sigma_{vel}^2$ and $(t-s_2)\varepsilon/\sigma_{vel}^2$ are evaluated with ε and σ_{vel}^2 for sources 1 and 2 respectively with $(t-s_1)$ and $(t-s_2)$ evaluated using the U for sources 1 and 2 respectively.

Source properties

For point sources we take $\sigma_{0x} = \max(t_R U, D_s)$ (which is infinite for continuous sources) and $\sigma_{0y} = \sigma_{0z} = D_s$. Here D_s is the source diameter and t_R is the release duration. For the continuous crosswind line sources and crosswind-vertical area sources which form the sub-source components of area, volume and line sources (which we only treat for continuous releases), we take σ_{0x} to be infinite, $\sigma_{0y} =$ source width divided by $\sqrt{12}$ and $\sigma_{0z} =$ source height range divided by $\sqrt{12}$. For multiple source cases (which again we only treat for continuous releases) we take the source separation vector $\sqrt{2}\mathbf{y}_\Delta$ to be (0, source separation in y direction, source separation in z direction). The effect of any along-wind separation of the sources is accounted for in the difference in travel times.

$\overline{c_m}$ and shape factors

For continuous releases we take:

$$\overline{c}_m = \max_{y,z} \overline{c}, h_z = \frac{\max_y \overline{c}}{\max_{y,z} \overline{c}} \text{ and } h_y = \frac{\overline{c}}{\max_y \overline{c}} \tag{36}$$

while for finite duration releases we take

$$\overline{c}_m = \max_{y,z,t} \overline{c}, \; h_z = \frac{\max_y \int \overline{c} dt}{\max_{y,z} \int \overline{c} dt}, \; h_y = \frac{\int \overline{c} dt}{\max_y \int \overline{c} dt} \tag{37}$$

and

$$h_x = \frac{\overline{c}}{h_y h_z \max_{y,z,t} \overline{c}} = \frac{\overline{c}}{\max_{y,z,t} \overline{c}} \frac{\max_{y,z} \int \overline{c} dt}{\int \overline{c} dt} \tag{38}$$

Here maxima over y are evaluated on the plume centre line and maxima over z are evaluated as maxima over the values at $z = 0$ and $z = z_p$. The time integrated concentration is taken equal to the concentration obtained from the 'plume' model

when run with source strength (release rate) numerically equal to the total mass released. The maxima over t are obtained as the minimum of (i) the plateau concentration for a long release with the same release rate and (ii) the value, for a puff release of duration zero and with the same total mass released, of the concentration at the time when the puff centre crosses the downwind distance of interest. For any location where any of the h factors exceed unity (this can happen because, for example, the maxima over $z = 0$ and $z = z_p$ are only approximations to the true maxima over all z) the maxima used in (36)-(38) are adjusted upwards to values which ensure all the h factors are less than or equal to unity.

σ_1 components

σ_{1x} is set to the value of σ_x from the mean concentration puff module. This is not the total puff length in that it does not include the spread resulting from the source size or source duration t_R. σ_{1y}^2 is taken to be the mean square plume spread from the mean concentration plume/puff module, excluding whatever source size addition is made in that module. However the σ_{yw}^2 part of σ_{1y}^2 is excluded when calculating $\sigma_{\Delta y}$. σ_{1z} for continuous releases is defined by $\overline{c}_m = \frac{Q}{2\pi U} \times$ (σ_y of actual plume) $\times$ (σ_{1z}^2 + addition for source size made in mean concentration module)$^{1/2}$, with a minimum of 10^{-3} m imposed. Q is the release *rate* here. For finite duration releases, σ_{1z} is calculated in the same way but with Q equal to total mass released and $\overline{c}_m$ replaced by $\max_{y,z} \int \overline{c} dt$.

4.2 Time averaging for continuous releases

We take $x_{av} = U t_{av}$. Here we evaluate U not at the mean plume height, but at the larger of the height of interest and z_b, where z_b is an estimate of the height at which the advective time for the plume fluctuation length scales is equal to the time for diffusion to the ground (see discussion in P13/01). z_b is calculated as

$$z_b \sim \frac{L_c \kappa^2}{\log((L_c \kappa^2 + z_0)/z_0)}$$

We take κ, von Karman's constant, equal to 0.4.

A further complication concerns σ_{yw} and σ_{yt}. We increase the σ_{1y} used to calculate $\sigma_{\Delta y}$ as follows

$$\sigma_{1y}^2 = \sigma_{yt}^2 + \sigma_{yw}^2 \max\left(1, t_{av}/t_{sample}\right)$$

This follows from the form of the default σ_{yw}^2 which is proportional to t_{sample} and the idea that contributions from sampling times up to t_{av} should appear as part of the t_{av} averaged plume width. If t_{av} and t_{sample} are both zero, we take t_{av}/t_{sample} =1. Of course σ_{yw} should be zero for t_{sample} =0.

4.3 Time integrated concentrations for finite duration releases

We treat this case for single point sources only. We adopt the reciprocity relation described in §3 and so implementation details follow those for single continuous point sources.

5. Interaction with other modules

The fluctuations module cannot be used with radioactivity, coastline, hills, plume chemistry or non-vertical jets. However it is designed to work with plume rise (vertical emission), deposition (wet and dry), plume visibility and (from ADMS 6) buildings.

Plume rise: This affects a number of input quantities through changes to the mean concentration field. In addition the plume spread due to plume rise is used to enhance σ_Δ. This follows the approach given by equation (4) of P13/05, but with source size not included in the enhancement as discussed in P13/06 and with changes necessitated by the new interpolation formula for σ_Δ. The final result is that we add σ_{pr}^2, the plume spread due to plume rise, to $\hat{R}^2$ (see equations (32) and (33).

Deposition: This is accounted for by changes in the $\overline{c}$ values and by the use of a source strength value that varies with downwind distance to account for deposition.

Plume visibility: This module may affect some variables input to the fluctuations module, but otherwise there is no interaction with fluctuations.

Buildings: Refer to P16/01.

The interaction with 'plumes above the boundary layer', which is not really a separate module but (in ADMS 3 onwards) an integral part of the basic dispersion model, also requires some comments. Only the 'in-boundary-layer' plume is treated and the source strength value supplied to the fluctuations module is depleted to reflect the loss of material through the boundary layer top (compare with deposition). The fact that any plume above the boundary layer is ignored should be borne in mind by users who make use of the fluctuation predictions away from the ground.

6. Summary of changes from ADMS 2

As a result of the modifications to treat multiple and anisotropic sources, the predictions with the new scheme are not always identical to those from the old scheme even in situations where the old scheme is applicable. The aspects which differ in situations where the old scheme was applicable are as follows:

- Separate y and z components are now used for quantities such as σ_1 and σ_Δ which indicate the spatial scales for the spread of particles and for the separation of particle pairs) and for the h, f and g factors (which indicate how the mean and mean square concentration vary spatially and how the mean square concentration at the location of the peak concentration is influenced by the spread in the various directions). Previously no distinction was made between the y and z directions for these quantities.
- The interpolation formula used for σ_Δ has been altered.
- The treatment of source size, σ_{yt} and σ_{yw} (the lateral spread due to turbulence and due to changes in the mean flow as predicted by the mean concentration module) has been rationalised in evaluating the particle spreads in the y and z directions, σ_{1y} and σ_{1z}, for use within the fluctuations module.
- All components of σ_Δ are used in calculating μ where appropriate (previously only the common value of the y and z components was used with $\sigma_{\Delta x}$ being left unused for instantaneous concentrations from finite duration releases).
- μ_A (the value of μ corresponding to idealised infinite sources) has been introduced into the calculation of μ. This can have an effect in situations where the old scheme was applicable because, for a small range of σ_Δ/σ_0 values (where σ_0 reflects the spatial scale of the source), the area source value μ_A is slightly greater than the line source value μ_L.
- For instantaneous concentrations from finite duration releases, the shape factors h_x, h_y, and h_z which indicate how the mean concentration falls off in the x, y and z directions are now calculated differently. The new approach avoids the use of $\max_t \overline{c}$ and uses more 'plume' quantities instead (i.e. quantities based on $\int \overline{c} dt$).
- The treatment of time averaging has been completely redesigned to provide for 'inertial-meander' subrange behaviour, to give a more rational treatment of the σ_{yw} term, and to allow the possibility of negative correlations between concentrations from different sources becoming more negative as averaging time increases.
- The clipped-normal pdf has been truncated at the 99.999th percentile (this change was anticipated in ADMS 2.2 for calculations of percentiles but not for calculations of probabilities).
- The plume rise induced spread is accounted for in calculating σ_Δ.

7. Tests and tuning of model constants

A number of tests were conducted, both to validate the model physics and to tune the model constants. The tests are limited in scope and further validation would be desirable; however they should give a good indication of model performance. Comparisons between the results presented here and those presented in P13/02 show reasonable agreement between the old and new schemes with only one case showing a significant difference (namely a somewhat different decay rate of concentration variance with averaging time – see figure 7 below and the equivalent figure in P13/02), but of course it must be remembered that the tests do not cover the entire range of possible scenarios.

The tests divide naturally into four categories: (i) tests of the downwind variation of $\sigma_c/\overline{c}$; (ii) tests of the crosswind variation of σ_c; (iii) tests of the two-source concentration correlation predictions for crosswind separated sources ; and (iv) tests of the time averaging procedure. In some of these tests there is a need to make assumptions about the mean concentration distribution – the fluctuations module requires information about the mean concentration field which is not always available in the experiments. Since we do not expect very precise agreement between the model and experimental data, we try to keep these assumptions simple (as in P13/02), even though this sometimes introduces some avoidable sources of error.

Before presenting results of the tests, we describe the procedure used to tune the constants A_0, A_1....A_5. All results presented below correspond to our preferred values for these constants. Note that A_1 affects only the multiple source results, and that A_2 to A_5 only affect results for non-zero time averaging. The first set of tests (the downwind variation of $\sigma_c/\overline{c}$) were used to tune the value of A_0. As anticipated in §3 a value somewhat less than the value of 2.0 used in ADMS 1 and 2 was needed to give optimum agreement, and the value 0.2 was judged to give best results. Note that the value of A_0 only affects results for downwind distances x corresponding to $x\varepsilon/U\sigma_{vel}^2$ of order unity or greater, and so the degree of agreement achieved for small x is achieved in effect without tuning. The second and third set of tests (the crosswind variation of σ_c and the two-source concentration correlations) were then carried out without any tuning. The concentration correlations do depend on the value of A_1, but quite reasonable agreement was achieved with our first guess value, $A_1 = 1$, and so no tuning was attempted. Note that, over the range of downwind distances for which we have correlation data, results are in fact insensitive to A_0 so the results shown have in effect been achieved without any tuning at all. The last set of tests (the effect of time averaging) were then carried out with the single source cases being used to tune the remaining constants. In fact there was insufficient data to justify tuning A_2 (this affects only the rate of decay of σ_c for small values of x and t_{av}) and the value of A_3 is not very important because μ decays to unity before the A_3 term dominates L_c (it could be more important if a smoother parameterisation were adopted for μ with μ reaching unity only asymptotically). Hence A_2 and A_3 were left equal to our first guess values of unity. Best results are judged to be given by $A_4 = 0.01$ and $A_5 = 0.02$. These may seem rather small for constants which are supposed to be of order unity, but in fact a little analysis shows that the decay of $\sigma_1^2 - \hat{\sigma}_\Delta^2$ towards zero as x_{av} increases occurs on a scale $A\sigma_{vel}^3/\varepsilon$ where A equals $A_0/\sqrt{A_4} = 2$

for small x and $1/\sqrt{3A_5} =$ 4.1 for large x – the values 2 and 4.1 seem more respectable for constants of order unity! Note that the agreement with the experimental data obtained in the inertial-meander subrange of the decay (the –1/3 slope seen in figure 6) is achieved without any tuning – the constants A_4 and A_5 only affect the behaviour outside this range.

7.1 Downwind variation of $\sigma_c/\overline{c}$

Here we compare the model with experimental data obtained by Mylne and Mason (1991), Mylne (1992), Mylne and Davidson (1996) and Fackrell and Robins (1982). The data in the first three references is atmospheric surface layer data and we concentrate attention on the near-neutral data. In calculating the model results we assume that $D_s = 0$ and $z_s/z_0 = 200$ (this value is not so appropriate for the data from the Sirhowy valley, Wales, but for the Sirhowy valley site one doesn't expect a normal surface layer and so it doesn't seem worthwhile to attempt a better estimate of z_0), that U, σ_u, σ_v, σ_w, and ε are given by standard surface layer forms (namely $(u_*/\kappa)\log((z+z_0)/z_0)$, $2.5u_*$, $2u_*$, $1.3u_*$ and $(u_*^3/\kappa z)$) and that $\overline{z}$ evolves as a function of travel time t according to Raupach's (1983) formula. σ_{1y} is taken to be $\sigma_v t$ (with changes in mean wind direction, σ_{yw}, set to zero, so that this value of σ_{1y} is used in all parts of the calculation – see §4.1) and two different assumptions are made for σ_{1z}. In the first assumption σ_z is given by Raupach's formula for $\overline{(z-\overline{z})^2}^{1/2}$ while in the second assumption σ_z is decreased by a factor of 0.627. The first assumption will be valid near the source while the second will be valid away from the source if $\overline{c}$ is a reflected Gaussian with $\overline{z}$ given by Raupach's formula. t and x are related by $x = U\big(\overline{z}(t)\big)t$. These assumptions are as in P13/02 except that separate assumptions are made here for σ_{1y} and σ_{1z}, reflecting the fact that the new scheme treats these quantities separately.

Figure 2 shows the downwind evolution of $\sigma_c/\overline{c}$ from the model (at the point of maximum $\overline{c}$) and as seen in the experiments (on the plume centreline in the horizontal and generally at source height, the exceptions being some measurements at 2 m for 1 m and surface releases). Because the model's $\overline{c}$ at the actual measurement point differs little from $\overline{c}_m$ (i.e. because $h_z \simeq 1$) the model predictions at the actual measurement point would not be very different. Two model curves are shown corresponding to the two assumptions about σ_{1z} discussed above. As well as the near-neutral experimental data, the results of Mylne's (1992) stable experiments are shown. The scaling adopted in figure 2 means the comparison with the stable data is appropriate near the source, but will be less appropriate when the plume's vertical spread is such that the height variation of U and ε (which of course is different in stable conditions) is significant.

In Fackrell and Robins (1982) wind tunnel data, the release height is above the surface layer and so a different approach is adopted. U, σ_u, σ_v, σ_w and ε are taken equal to their values at the source height and σ_{1y}^2 and σ_{1z}^2 are calculated using

$$\sigma_{1y}^2 = \sigma_v^2 t^2 / \max(1, 2.58 t\varepsilon/\sigma_{vel}^2) \qquad (39)$$

and

$$\sigma_{1z}^2 = \sigma_w^2 t^2 / \max(1, 2.58 t\varepsilon/\sigma_{vel}^2). \qquad (40)$$

These expressions are chosen to equal $\sigma_v^2 t^2$ and $\sigma_w^2 t^2$ for small t and to have the same dependence on travel time as the reciprocal of the observed $\overline{c}_m$. Changes in mean wind direction are set to zero and D_s is taken equal to the source diameter. These assumptions are as in P13/02 except that separate assumptions are made here for σ_{1y} and σ_{1z}.

The results of the comparison are shown in figure 3 for various source sizes. The model results show $\sigma_c/\overline{c}$ at the point of maximum $\overline{c}$ while the quantity measured by Fackrell and Robins was peak σ_c divided by peak $\overline{c}$ (i.e. the two quantities are not necessarily measured at the same point). Although this introduces some errors into the comparison, the model predictions of σ_c vary little between the locations of the observed peaks in σ_c and in $\overline{c}$. In fact the model shows much less variation of σ_c between these locations than is seen in the experiments, the experiments showing a decrease in σ_c as the ground is approached when the maximum in $\overline{c}$ is at the ground. Such a decrease was not however observed by Mylne (1993) during atmospheric (as opposed to wind tunnel) studies. At large travel times the above assumptions about , σ_u, σ_v, σ_w and ε are not accurately valid and an attempt has been made to assess the error at the largest times plotted in figure 3. Taking $\overline{z}$ as $0.3H$ (in Fackrell and Robins' notation) and evaluating the mean flow and turbulence properties at height $\overline{z}$ implies an increase in the model prediction of $\sigma_c/\overline{c}$ of about 30% at the largest times plotted.

7.2 Crosswind variations of σ_c

Here we compare with data from Mylne and Mason's (1991) figure 9(a). In addition to the data given in Mylne and Mason's figures 8 and 9(a) we need to make assumptions about the flow and we adopt the same assumptions as made for the atmospheric experiments in §7.1 (indeed we make use of these assumptions in all the atmospheric experiments considered throughout §7, using either the near source or far downwind assumptions about σ_{z1} as appropriate). It is not clear from Mylne and Mason's paper what value $x\varepsilon/U\sigma_{vel}^2$ takes; however from the value of x given we estimate $x\varepsilon/U\sigma_{vel}^2$ to be of order 15. Note that model results here are insensitive to $x\varepsilon/U\sigma_{vel}^2$, for $x\varepsilon/U\sigma_{vel}^2 \gg 1$ with the model evolving self-similarly at large x. The comparison between model and experimental results is shown in figure 4.

7.3 Two-source correlations

The scheme was tested against the two-source experiments carried out in the atmospheric surface layer at Cardington by Davies *et al.* (1998). In these experiments the correlation between the concentration resulting from two sources separated in the crosswind direction was measured. Figure 5 shows a comparison between the model and experimental values of the correlation as a function of downwind distance x and source separation Δy. The model results are evaluated on the centreline running downwind from the point midway between the two sources while the experimental results are at the height of the sources but at a variety of crosswind positions. The

pattern of the experimental results shows little change however if we include only measurements obtained close to the centreline.

7.4 Effect of time averaging

The time averaging scheme was tested against the results from the experiments by Mylne and Mason (1991) and Davies *et al.* (1998). Figure 6 shows the decay of $\sigma_c/\overline{c}$ with averaging time from the model (at the point of maximum $\overline{c}$) and as seen in the experiments of Davies *et al.* (at source height and close to the plume centreline in the horizontal – see Davies *et al.* for the precise criteria for accepting measurements as being 'close to the centreline'). The two curves plotted correspond to $x\varepsilon/U\sigma_{vel}^2$ values of 0.02 and 0.2, which span the range of the measurements. Note that an inertial meander subrange (-1/3 slope) can be clearly seen and that results for the two curves converge in this subrange and become independent of x. This is expected because in this range the t_{av}-averaged plume width becomes proportional to travel time, and so $\hat{\sigma}_\Delta^2/\sigma_1$ which characterises the fraction of plume spread due to meandering, becomes independent of travel time. The graph suggests that the values of σ_c obtained in the experiments may be suffering a little from instrument frequency response at the smallest values of x.

Figure 7 shows a comparison of the model with the data on the effect of time averaging given in figure 5 of Mylne and Mason (1991). The experimental data were obtained at source height but at a position off the centreline in the horizontal at $y/\sigma_{1y} \simeq 1$ while the model results were obtained with $h_y = \exp(-1/2)$ (reflecting the off-axis position of the observation) and $h_z = 1$. The value of $x\varepsilon/U\sigma_{vel}^2$ (for model and experiment) was about 3.3.

Finally figure 8 shows the effect of averaging time on the two-source concentration correlations. This shows the magnitude of both the positive and negative correlations increasing with averaging time, but with the dividing line between the positive and negative correlations moving so that some of the negative correlations became positive. This agrees qualitatively with the results found by Davies *et al.* (1998).

References

Batchelor, G.K., 1952, 'Diffusion in a field of homogeneous turbulence II. The relative motion of particles', *Proc. Camb. Phil. Soc.,* **48**, 345-362.

Davies, B.M., Jones, C.D., Manning, A.J. and Thomson, D.J., 1998, 'Some field experiments on the interaction of plumes from two sources', Internal Met. Office note, TDN 252.

Durbin, P.A., 1980, 'A stochastic model of two–particle dispersion and concentration fluctuations in homogeneous turbulence', *J. Fluid Mech.,* **100**, 279-302.

Fackrell, J.E. and Robins, A.G., 1982, 'Concentration fluctuations and fluxes in plumes from point sources in a turbulent boundary layer', *J. Fluid Mech.,* **117**, 1-26.

Gifford, F., 1959, 'Statistical properties of a fluctuating plume dispersion model', *Adv. Geophys.,* **6**, 117-137.

Mylne, K.R., 1992, 'Concentration fluctuation measurements in a plume dispersing in a stable surface layer', *Boundary–Layer Meteorol.,* **60**, 15-48.

Mylne, K.R., 1993, 'The vertical profile of concentration fluctuations in near-surface plumes', *Boundary-Layer Meteorol.,* **65**, 111-136.

Mylne, K.R., Davidson, M.J. and Thomson, D.J., 1996, 'Concentration fluctuation measurements in tracer plumes using high and low frequency response detectors', *Boundary-Layer Meteorol.,* **79**, 225-242.

Mylne, K.R., and Mason, P.J., 1991, 'Concentration fluctuation measurements in a dispersing plume at a range of up to 1000m', *Q. J. R. Meteorol. Soc.,* **117**, 177-206.

Raupach, M.R., 1983, 'Near-field dispersion from instantaneous sources in the surface layer', *Boundary-Layer Meteorol.,* **27**, 105-113.

Sawford, B.L., 1983, 'The effect of Gaussian particle-pair distribution functions in the statistical theory of concentration fluctuations in homogeneous turbulence', *Q. J. R. Meteorol. Soc.,* **109**, 339-354.

Sykes, R.I., 1984, The variance in time-averaged samples from an intermittent plume, *Atmos. Environ.,* **18**, 121-123.

Thomson, D.J., 1990, 'A stochastic model for the motion of particle pairs in isotropic high-Reynolds-number turbulence, and its application to the problem of concentration variances', *J. Fluid Mech.,* **210**, 113-153.

Thompson, D.J., 1997, 'The "inertial-meander" subrange of a dispersing plume', *J. Appl. Met.,* **36**, 1046-1049.

Townsend, A.A., 1954, ‘The diffusion behind a line source in homogeneous turbulence’, *Proc. Roy. Soc.*, A, **224**, 487-512.

1(a)

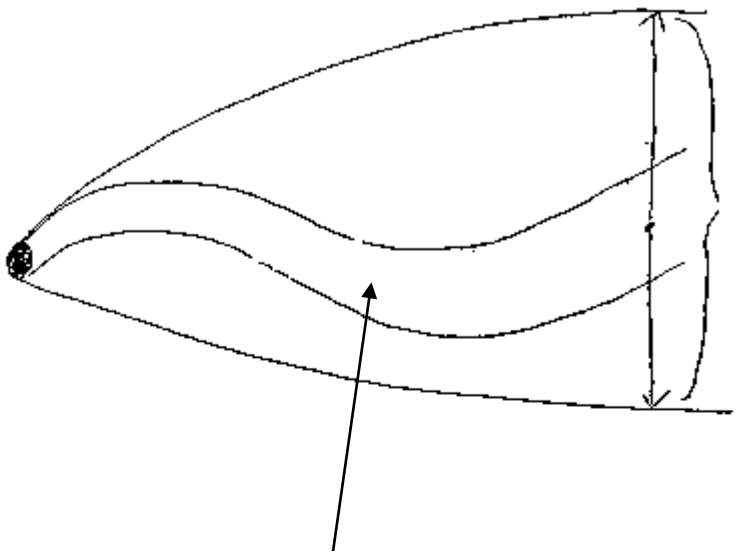

1(b)

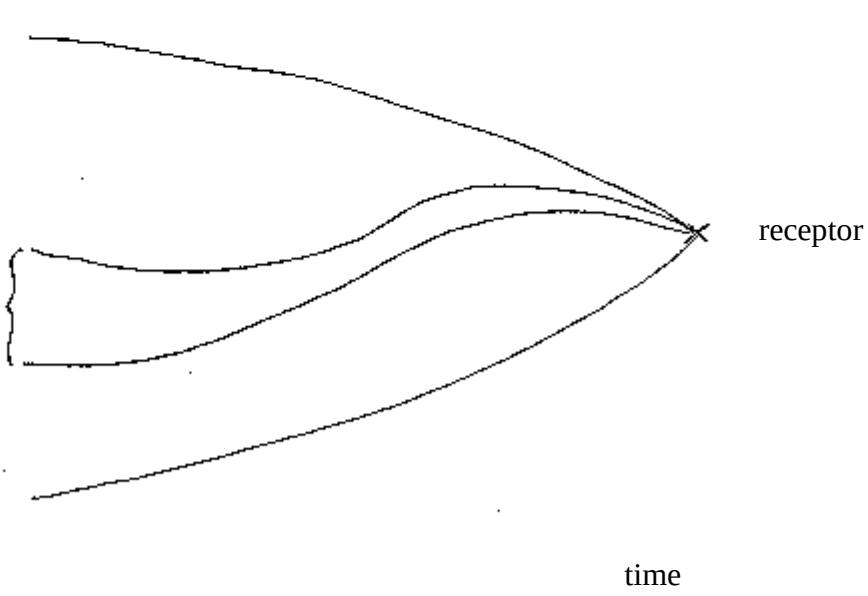

Figure 1: Illustration of Gifford's meandering plume (or puff) model. Figure 1 (a) shows the usual forward-in-time model, while figure 1(b) shows the backwards model. In the backwards model, the plume or puff does not refer to a real plume or puff of pollutants, but simply indicates the region from which the material observed at the receptor is drawn. If, at any given instant, the sources lie within the instantaneous backwards plume, then the material emitted at that time will contribute to the observed concentration at the receptor.

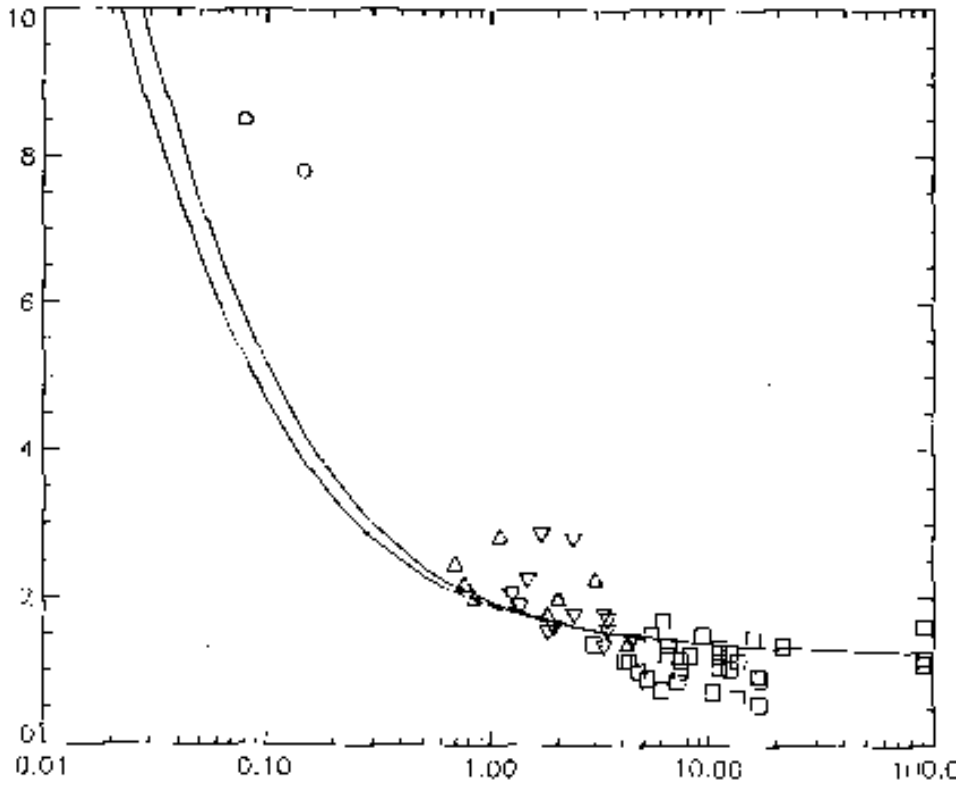

x

Figure 2: Plot of $\sigma_c/\overline{c}$ as a function of downwind distance x, with x scaled by ε, U and σ_{vel}^2 evaluated at source height. The lines show the model predictions corresponding to the two assumptions made about σ_{1z} while the symbols show the results of the field experiments. Squares and inverted triangles denote experiments carried out in the Fens and in South Wales respectively (Mylne and Mason 1991), triangles denote experiments conducted in stably stratified conditions at Cardington (Mylne 1992), and circles denote very short range Cardington experiments (Mylne *et al.* 1996). The results for surface releases (for which $x\varepsilon/U\sigma_{vel}^2$ is infinite) are plotted at $x\varepsilon/U\sigma_{vel}^2$ =90.

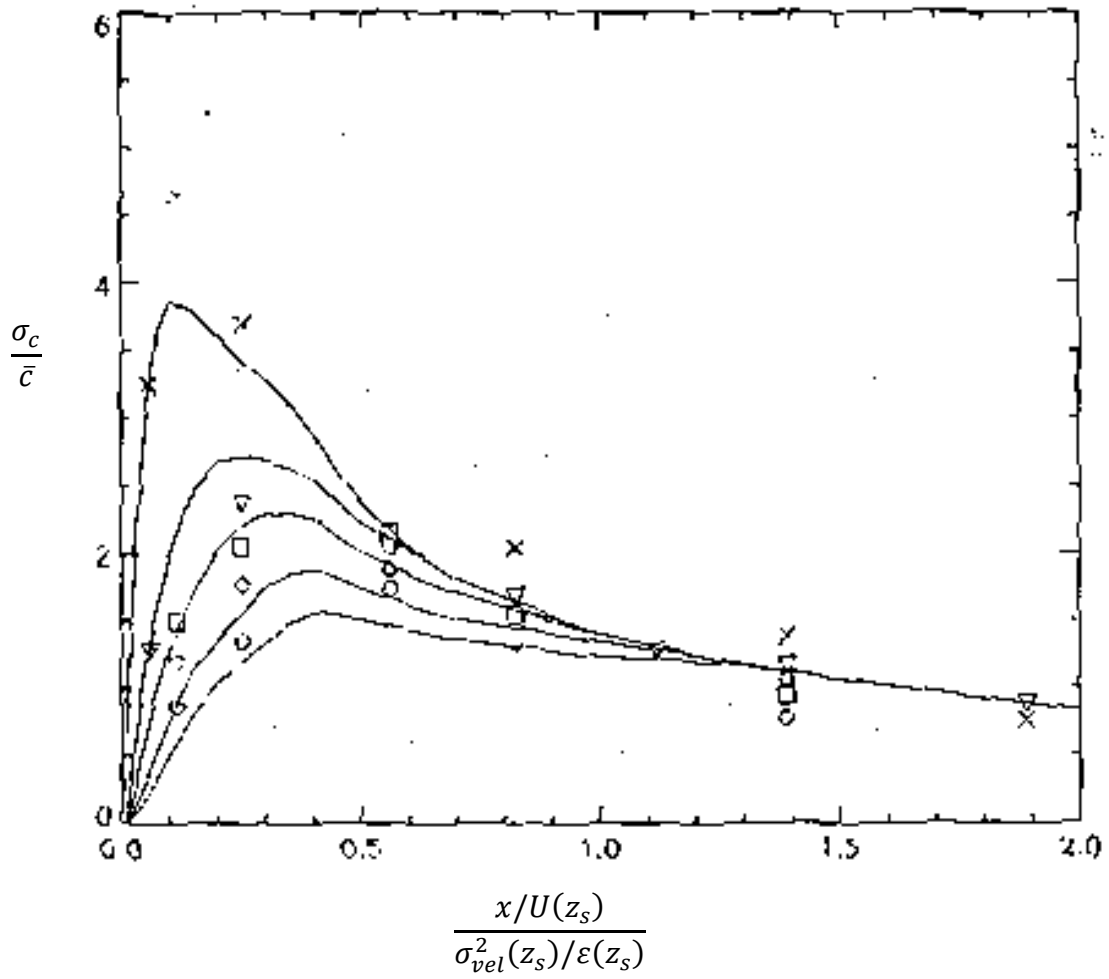

Figure 3: Plot of $\sigma_c/\bar{c}$ as a function of downwind distance x for various source sizes, with x scaled by ε, U and σ_{vel}^2 evaluated at source height. The lines show the model predictions while the symbols show the laboratory experiments of Fackrell and Robins (1982).

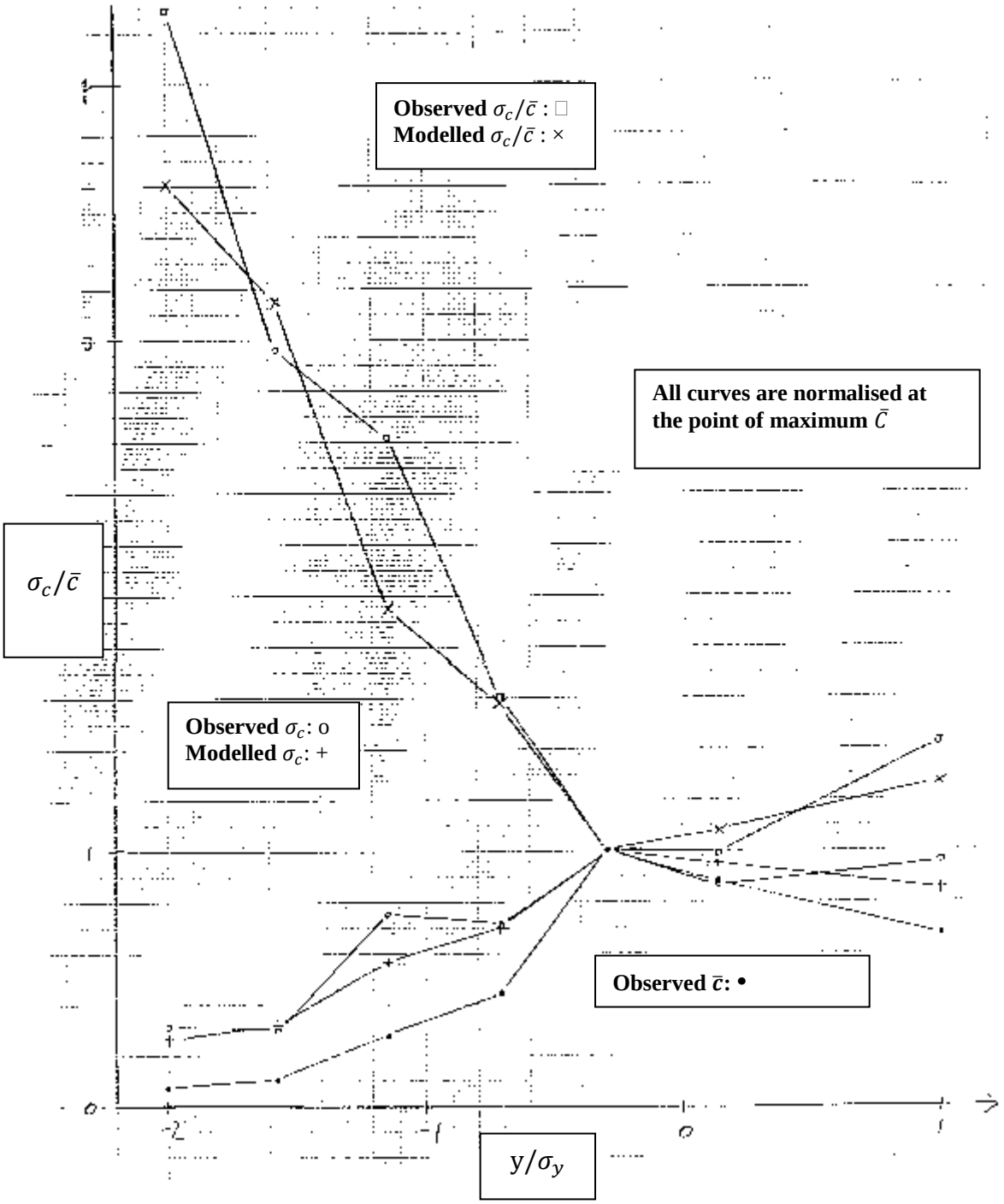

Figure 4: Crosswind variation of the plume properties for the case given in figure 9(a) of Mylne and Mason (1991). The symbols are as follows: solid circles, observed $\overline{c}$; open circles, observed σ_c; squares, observed $\sigma_c/\overline{c}$; +, modelled σ_c; ×, modelled $\sigma_c/\overline{c}$. All curves are normalised by their values at the point where $\overline{c}$ is a maximum.

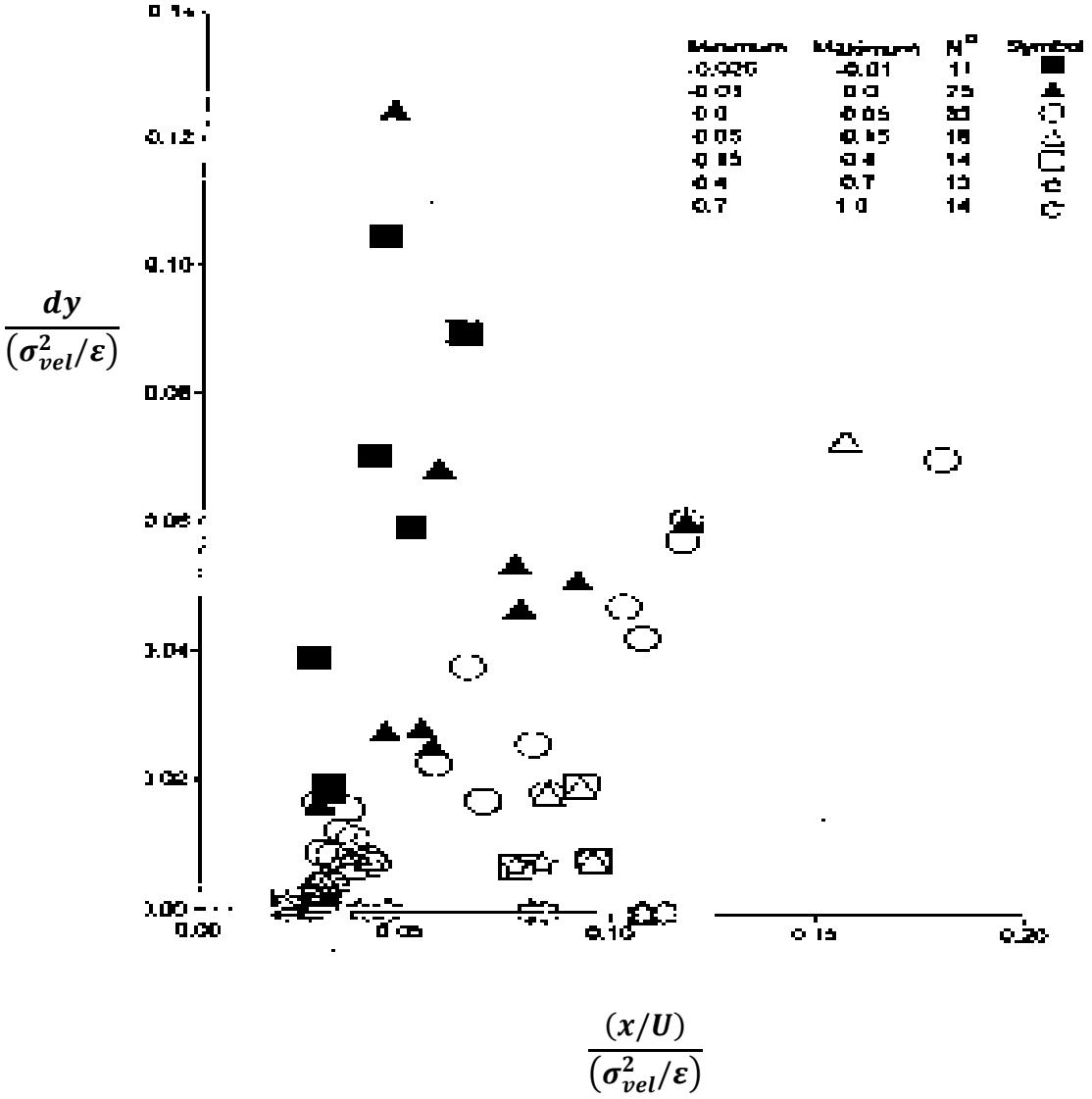

Figure 5a: Correlation between the concentrations at downwind distance x resulting from two sources separated in the crosswind direction by a distance Δy. x and Δy are scaled with ε, U and σ_{vel}^2 evaluated at source height. Figure 5a shows the experimental data of Davies *et al.* (1998).

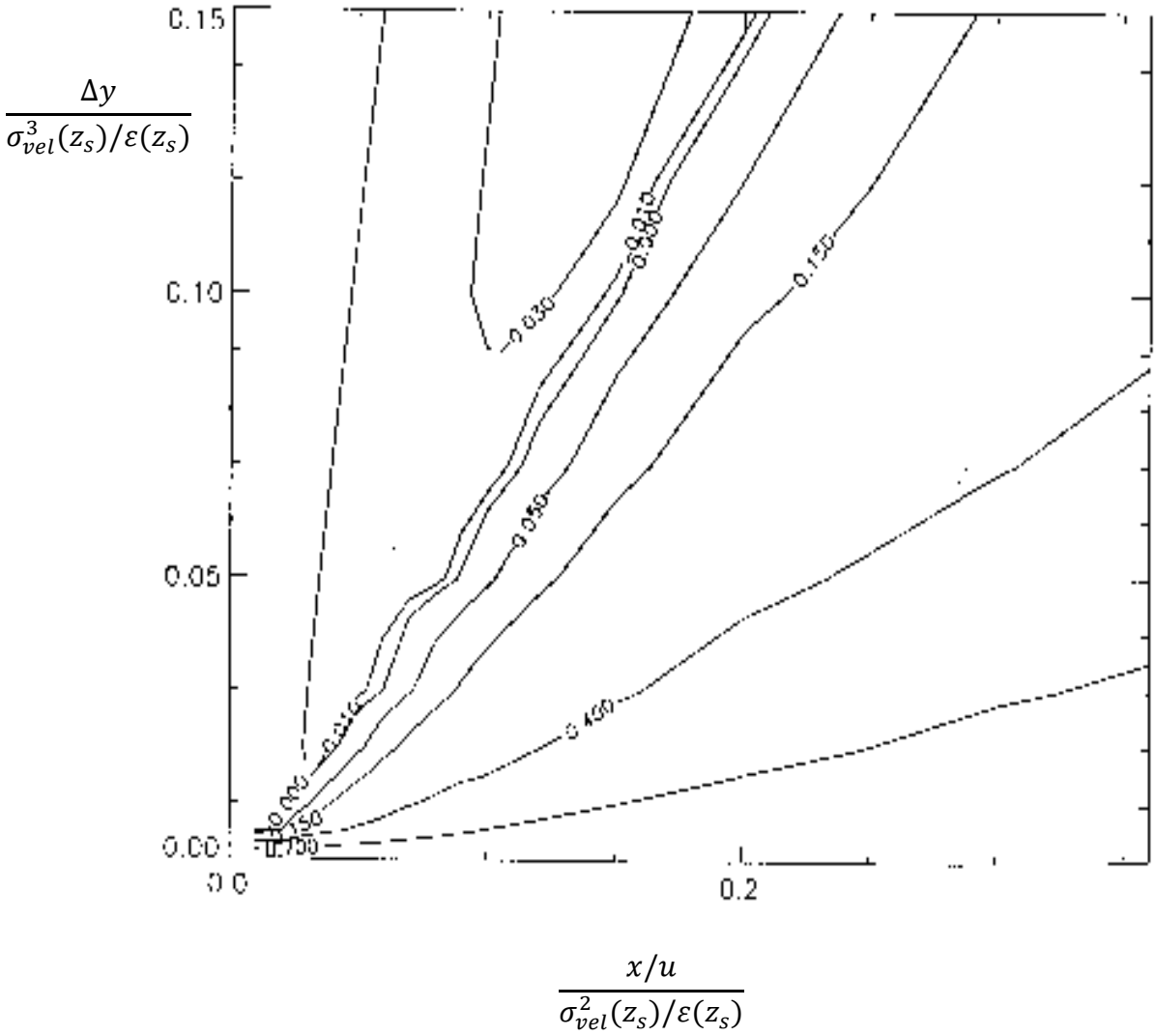

Figure 5b: Correlation between the concentrations at downwind distance *x* resulting from two sources separated in the crosswind direction by a distance Δy. x and Δy are scaled with ε, U and σ_{vel}^2 evaluated at source height. Figure 5b shows the model results.

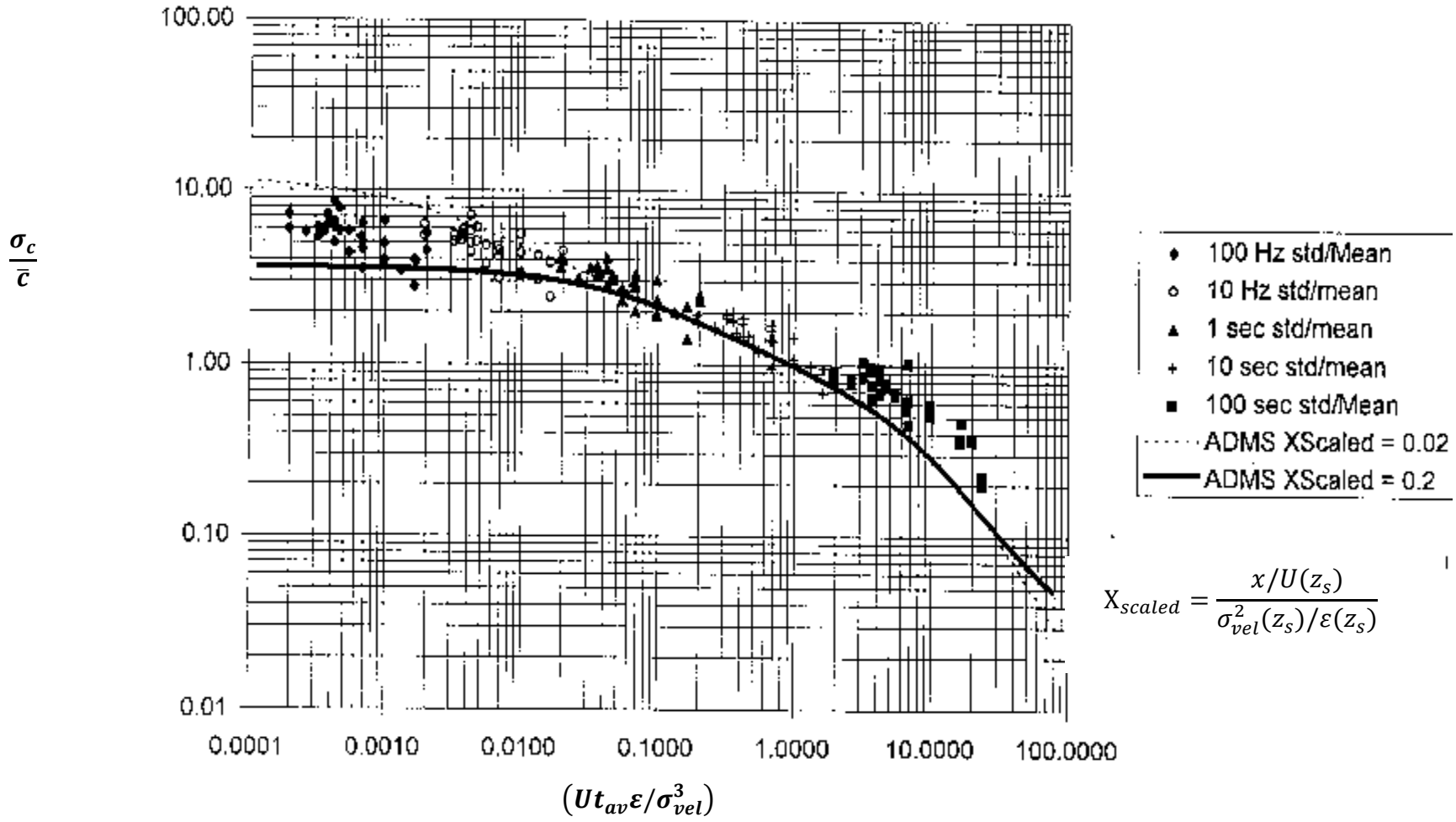

Figure 6: Effect of averaging time on σ_c. The symbols show the experimental data of Davies *et al.* (1998) while the lines show the model results for $x\varepsilon/U\sigma_{vel}^2$ =0.02 and 0.2 with ε, U and σ_{vel}^2 evaluated at source height (these values span the range of values in the experiments). t_{av} is scaled with ε, U and σ_{vel}^2 evaluated at source height.

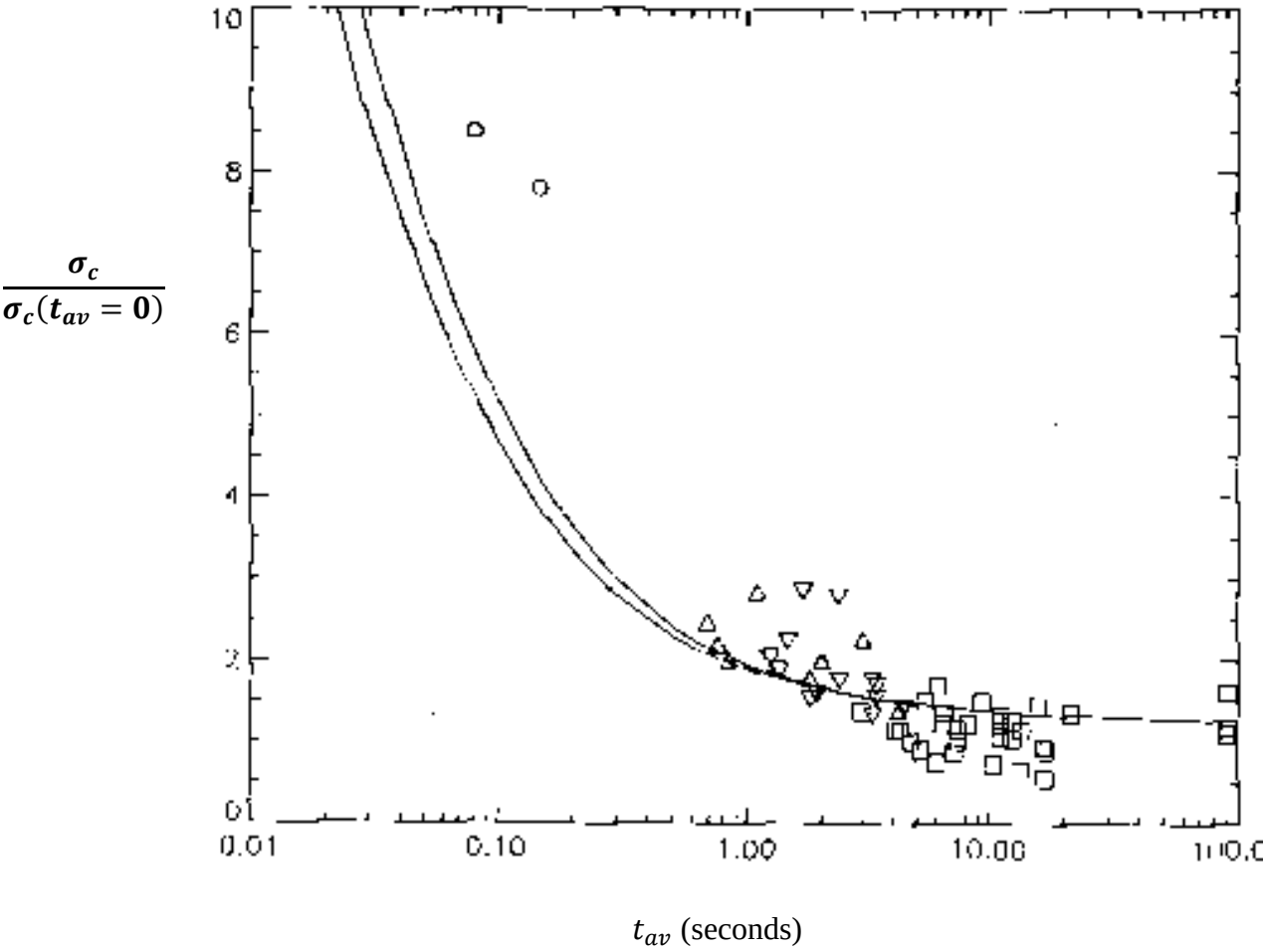

Figure 7: Effect of averaging time on σ_c for the case given in figure 5 of Mylne and Mason (1991). The symbols show the experimental data while the line shows the model results

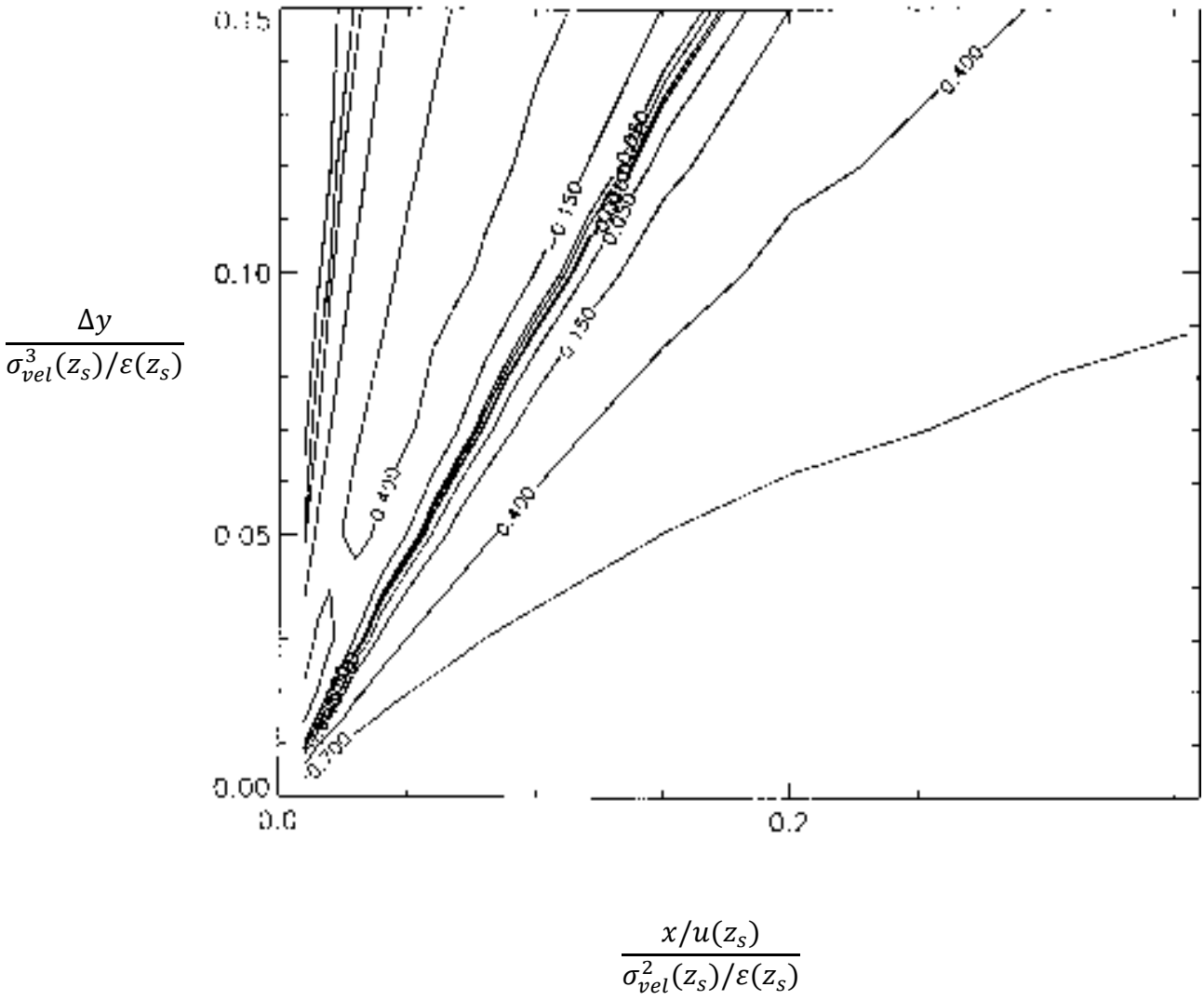

Figure 8: The effect of averaging time on the two-source concentration correlations. This shows the same information as in figure 5 but for a value of $t_{av}U\varepsilon/\sigma_{vel}^3$ of 1 (with ε, U and σ_{vel}^2 evaluated at source height).